ARCHIVES OF MECHANICS
Arch. Mech. **77** (4), 401–429, 2025, https://doi.org/10.24423/aom.4700

Analytical solution of peridynamics for heat conduction with an external source

S. FAN[1)], H. LIU[2)], X. PENG[2*)]

[1)] *School of Mechanics and Construction Engineering, Key Laboratory of Green Toughening and Safety Prevention and Control of Offshore Structures, Jinan University, Guangzhou 510632, China*

[2)] *Department of Engineering Mechanics, School of Aerospace Engineering, Huazhong University of Science and Technology, Wuhan, 430074, China, e-mail*[*)]*: peng.x.h@foxmail.com (corresponding author)*

This study provides a novel analytical approach for solving one- and two-dimensional heat conduction problems with an external heat source within the peridynamic framework. By employing Duhamel's principle, the inhomogeneous governing equation with an external source is transformed into a homogeneous equation, enabling the derivation of peridynamic analytical solutions through separation of variables. An innovation involves introducing a nonlocal factor by ensuring compatibility between the spatial functions in the peridynamic solution and their classical continuum mechanics counterparts. Numerical examples demonstrate the methodology's effectiveness for both one- and two-dimensional heat conduction problems subjected to sinusoidal and constant external sources, and the nonlocal effect is measured based on the nonlocal factor. Unlike peridynamic systems without external sources, these examples reveal that the nonlocal factor appears not only in the exponential term but also in other components of the solution, indicating persistent nonlocal effects even as time approaches infinity. Furthermore, the analysis shows that the kernel function with $n = 0$ exhibits the strongest nonlocal influence, while $n = 2$ results in the weakest nonlocal behavior. The findings demonstrate that peridynamic analytical solutions for heat conduction can be systematically derived from classical continuum mechanics solutions through appropriate incorporation of the nonlocal factor. This work significantly expands the scope of peridynamic analytical solutions and offers new insights into nonlocal heat conduction phenomena, providing a valuable foundation for future studies in this field.

Key words: peridynamics, heat conduction, analytical solution, nonlocal effect.

1. Introduction

The nonlocal theory involving integral formulations of the classical continuum mechanics media has been established since the 1960s. In its early development, Kröner added a nonlocal integral term to the local equations of motion [1], Eringen and Edelen proposed a nonlocal theory of elasticity

expressed in terms of integral constitutive relations [2, 3], and Kunin put forward the general model of an inhomogeneous elastic medium of a simple structure with nonlocal interaction [4].

Recently, Silling has proposed a nonlocal theory called peridynamics, which is actually an integral nonlocal model [5]. Unlike other nonlocal models, peridynamics only considers the displacement field, not the displacement gradient [6]. Therefore, one of the attractive features of peridynamics is the advantage due to the absence of spatial gradients, especially in the case of problems involving discontinuities, such as fracture [7–11], impact [12–14], corrosion [15–20], fatigue [21–24], and so on.

The horizon parameter δ serves as a fundamental length scale in peridynamics, governing both the equation of motion and constitutive relations by defining the maximum interaction range between material particles [25]. Emmrich and Weckner have proved that the bond-based peridynamic will converge to the classical elasticity when the horizon δ goes to zero [26]. And to the state-based peridynamics, Silling and Lehoucq have verified that the peridynamic operator converges to the classical operator if the deformation is classically smooth with the limitation of horizon δ, which means that the state-based peridynamics also converges to the classical elasticity when the horizon δ approaches zero [27]. This means that the peridynamic theory can coincide with the classical continuum mechanics when the horizon δ goes to zero. Therefore, since the horizon δ can be recognized as the nonlocal measure, it plays a crucial role in peridynamics.

Peridynamics reformulates continuum mechanics problems by replacing differential operators with integral equations, thereby eliminating spatial derivatives but introducing significant challenges for analytical solution methods. This mathematical transformation fundamentally alters the solution approach, making most practical problems solvable only to numerical treatment. Nevertheless, analytical solutions remain attainable for certain idealized cases, providing crucial validation for numerical schemes and key physical intuition about nonlocality. Silling *et al.* studied the deformation of the infinite rod with a point load and obtained the series solution [28]. Weckner put forward the three-dimensional peridynamic Green function with the Laplace transformation and the Fourier transform, giving the integral solution of the three-dimensional peridynamics [6, 29]. Mikata *et al.* analytically treated the peristatic and peridynamic problems for a one-dimensional infinite rod and studied the dispersion curves and group velocities for the materials with three different micromoduli [30]. Wang *et al.* verified that the Green function can be uniformly expressed as the superposition of three parts, namely conventional solution, the Dirac function, and converge nonlocal integration [31]. Hang *et al.* analyzed one-dimensional uniaxial elongation analytically with peridynamics [32]. Zhao *et al.* provided an analytical approach to analyze the vibration of a peridynamic

finite bar with specified boundary conditions, proving that the nonlocal dispersive relation of the peridynamic bar is nonlinear [33]. However, there is an error between the peridynamic analytical solution and classical continuum mechanics solution due to the nonlocal effect [34], some criteria must be proposed to measure the strength of the nonlocal effect.

Nowadays, Chen *et al.* put forward a new way of obtaining the peridynamic analytical solution of heat conduction in a finite domain based on the mathematical methods for physics [35]. Through the introduction of a nonlocal factor, the authors established quantitative criteria for assessing nonlocal effects and demonstrated that peridynamic analytical solutions can be systematically derived by incorporating this factor into the exponential terms of classical continuum mechanics solutions. Their approach generates highly convergent series solutions, offering a powerful extension to analytical methods in peridynamics without sacrificing computational feasibility or physical clarity. In their foundational work, the authors addressed the homogeneous heat conduction equation, which inherently excludes consideration of the external heat source. However, numerous practical heat conduction phenomena involve external thermal excitation, leading to fundamentally different physical behavior compared to source-free systems. This critical distinction necessitates dedicated investigation of non-homogeneous heat conduction problems to properly account for external source effects.

This paper investigates nonhomogeneous heat conduction problems incorporating the external heat source within the peridynamic framework. In contrast to conventional homogeneous formulations, the presence of an external heat source introduces fundamental modifications to the governing equations, manifesting as nonhomogeneous terms that significantly alter the system's thermal response characteristics. The content of this article is organized as follows: In Section 2, we analyze the one-dimensional heat conduction problem with the sinusoidal external heat source and give the peridynamic analytical series solution. In Section 3, we further study the two-dimensional heat conduction problem also with the constant external heat source and obtain its peridynamic analytical series solution. In Section 4, some useful conclusions are drawn.

2. Analytical solution for one-dimensional nonlocal heat conduction with an external heat source in a finite domain

2.1. One-dimensional classical heat conduction equation

Heat conduction represents a fundamental transport phenomenon that occurs when thermal energy transfers from regions of higher temperature to areas of lower temperature within a material body due to spatial temperature gradients. In this process, temperature is a function of space and time. The governing partial

differential equation, commonly referred to as the heat equation, describes the temporal and spatial evolution of this temperature field. Analytical or numerical solutions to this equation provide a complete characterization of the transient thermal distribution throughout the material domain.

The classical one-dimensional heat conduction equation with an external source can be written as:

$$\frac{\partial \Theta(x,t)}{\partial t} = D\frac{\partial^2 \Theta(x,t)}{\partial x^2} + f(x,t), \tag{2.1}$$

where $\Theta(x,t)$ is the temperature related to space and time, and it can also be the concentration in mass diffusion problem; $f(x,t)$ is the external heat source related to space and time; D is the thermal diffusion coefficient or the material diffusivity in mass diffusion problem.

When we study the heat insulation-dissipative system, the boundary conditions in one-dimension are denoted as:

$$\Theta(0,t) = 0, \quad \frac{\partial \Theta(L,t)}{\partial x} = 0, \quad t > 0, \tag{2.2}$$

where $x = 0$ and $x = L$ define the boundaries of the one-dimensional finite domain, representing the left and right extremities, respectively. And when the temperature is zero everywhere in the initial moment, the initial condition is written as:

$$\Theta(x,0) = 0. \tag{2.3}$$

These above three equations constitute the insulation-dissipative system in one-dimensional heat conduction problem we study in Section 2.

According to Duhamel's principle [36], the above inhomogeneous equation (2.1), the boundary conduction (2.2), and the initial condition (2.3) can be expressed as:

$$\begin{cases} \frac{\partial w}{\partial t} = D\frac{\partial^2 w}{\partial x^2}, & 0 < x < L,\ t > \tau, \\ w(0,t) = 0,\ \frac{\partial w(L,t)}{\partial x} = 0, & t > \tau, \\ w(x,\tau) = f(x,\tau), & 0 < x < L, \end{cases} \tag{2.4}$$

where $w(x,t;\tau)$ is the intermediate variable about space and time at $t = \tau$, which satisfies:

$$\Theta(x,t) = \int_0^t w(x,t;\tau)\, d\tau. \tag{2.5}$$

To verify such equivalence between Eqs. (2.1)–(2.3) and Eqs. (2.4) and (2.5), one can first take the derivative of time t and space x about Eq. (2.5), which yields:

$$\frac{\partial\Theta}{\partial t} - D\frac{\partial^2\Theta}{\partial x^2} = w(x,t;\tau)|_{\tau=t} + \int_0^t \frac{\partial w(x,t;\tau)}{\partial t}\,d\tau - D\int_0^t \frac{\partial^2 w(x,t;\tau)}{\partial x^2}\,d\tau = f(x,t). \tag{2.6}$$

Equation (2.6) shows that Eq. (2.5) meets the heat conduction equation in Eq. (2.1). When it comes to the boundary condition, it is concluded that:

$$\begin{aligned} \Theta(0,t) &= \left[\int_0^t w(x,t;\tau)\,d\tau\right]_{x=0} = \int_0^t w(x,t;\tau)|_{x=0}\,d\tau = 0, \\ \frac{\partial\Theta(L,t)}{\partial x} &= \left[\int_0^t \frac{\partial w(x,t;\tau)}{\partial x}\,d\tau\right]_{x=L} = \int_0^t \frac{\partial w(x,t;\tau)}{\partial x}\bigg|_{x=L} d\tau = 0. \end{aligned} \tag{2.7}$$

This means that the solution in Eq. (2.5) can satisfy the boundary condition in Eq. (2.2). Finally, in order to verify the initial conditions, we have:

$$\Theta(x,0) = \int_0^0 w(x,t;\tau)d\tau = 0. \tag{2.8}$$

So far, we have turned the inhomogeneous Eq. (2.1) into the homogeneous Eq. (2.4), and verified their equivalence in the governing equation, boundary condition, and initial condition. It should be noted that the basis of Duhamel's principle lies in the impulse theorem, which states that the impulse caused by the action of a force is equal to the change in momentum. Therefore, Duhamel's principle can only be used for developing physical processes, not for stable ones. Then the homogeneous governing equation of heat conduction with an external source is solved based on the method of separation of variables in the mathematical method of physics.

2.2. Peridynamic analytical solution for one-dimensional heat conduction in a finite domain

Obtaining analytical solutions for peridynamic integral equations generally presents significant mathematical challenges. Nevertheless, the heat conduction problem in peridynamics admits potential analytical treatment through strategic formulation. The key insight lies in the transformability of the nonhomogeneous

governing equation (Eq. (2.1), Section 2.1) with external source terms into its homogeneous counterpart (Eq. $(2.4)_1$). This crucial reduction enables derivation of analytical solutions for externally-driven peridynamic systems by building upon the fundamental solutions of the homogeneous equation. Corresponding to the classical heat conduction Eq. $(2.4)_1$, the heat conduction equation in peridynamics is expressed in its integral form as [35]:

$$\frac{\partial \Theta(x,t)}{\partial t} = DL_\delta \Theta(x,t), \tag{2.9}$$

where L_δ stands for the peridynamic Laplacian operator, written by

$$L_\delta \Theta(x,t) = \int_{H_{\boldsymbol{x}}} \mu(|\hat{\boldsymbol{x}} - \boldsymbol{x}|)[\Theta(\hat{\boldsymbol{x}},t) - \Theta(\boldsymbol{x},t)]\, dV_{\hat{\boldsymbol{x}}}, \tag{2.10}$$

and $H_{\boldsymbol{x}}$ and δ denote the horizon region and horizon size, respectively; $\mu(|\hat{\boldsymbol{x}}-\boldsymbol{x}|)$ is the kernel function. And the integral is evaluated over the whole horizon region.

According to the mathematical methods of physics, the homogeneous partial differential equation (2.4) in classical continuum mechanics can be solved by the separation of variables, which inspires us that we may deal with the peridynamic heat conduction integral equation similarly. First, we assume that Eq. (2.9) also has a formal solution with separate variables as:

$$\Theta(x,t) = X(x)T(t). \tag{2.11}$$

Substituting Eq. (2.11) into Eq. (2.9) gives the following result:

$$\frac{L_\delta X(x)}{X(x)} = \frac{1}{D}\frac{T'(t)}{T(t)} = C, \tag{2.12}$$

where C is the separation constant, and in peridynamics, this separation constant is related to the horizon size δ which is denoted as Ψ^δ, namely

$$C = \Psi^\delta. \tag{2.13}$$

With Eq. (2.12) and Eq. (2.13), one can obtain the following ordinary differential equation and the other integral equation as:

$$\begin{cases} T'(t) - D\Psi^\delta T(t) = 0, \\ L_\delta X(x) - \Psi^\delta X(x) = 0. \end{cases} \tag{2.14}$$

Relative to the complex integral equation, the ordinary differential equation in Eq. $(2.14)_1$ is much easier to solve and its general solution is:

$$T(t) = \begin{cases} A_1, & \Psi^\delta = 0, \\ A_2 \mathrm{e}^{D\Psi^\delta t}, & \Psi^\delta \neq 0, \end{cases} \tag{2.15}$$

where A_1 and A_2 are both arbitrary constants.

Now turning to the second integral equation $(2.14)_2$, an examination of the solution procedure for the classical heat conduction equation via the separation of variables method may provide insights for its resolution. First, in the mathematical method of physics, the solution of the homogeneous heat conduction equation, for example, Eq. (2.1) without the inhomogeneous term, can be obtained with the separation of variables as [35]:

$$X^c(x) = \begin{cases} Gx + H, & \Psi^c = 0, \\ I \sin kx + J \cos kx, & \Psi^c \neq 0, \end{cases} \tag{2.16a}$$

$$T^c(t) = \begin{cases} E, & \Psi^c = 0, \\ F\mathrm{e}^{D\Psi^c t}, & \Psi^c \neq 0, \end{cases} \tag{2.16b}$$

where G, H, I, J, k are arbitral constants; and $\Psi^c = -k^2$ is the separation constant for the classical heat conduction equation, the same tackle as it is done in the peridynamic heat conduction of Eqs. (2.12) and (2.13). Then we see that Eq. (2.16a) satisfies Eq. $(2.14)_2$ for $\Psi^c = 0$ [35], which inspires us that once solution (2.16a) with $\Psi^c \neq 0$ satisfies Eq. $(2.14)_2$, we may find the connection of peridynamics and the classical heat conduction problem, and further give the peridynamic analytical heat conduction solution with an external source.

For nonzero Ψ^δ, we assume Eq. (2.16a) satisfies $(2.14)_2$, and then making the substitution. For the equation to hold after the above substitution, the following relationship must be satisfied:

$$\Psi^\delta = \hat{\mu}_k - \beta^\delta = \int_{-\delta}^{\delta} \mu(|\boldsymbol{\xi}|) \cos(k\boldsymbol{\xi}) d\boldsymbol{\xi} - \int_{-\delta}^{\delta} \mu(|\boldsymbol{\xi}|)\, d\boldsymbol{\xi}, \tag{2.17}$$

where $\boldsymbol{\xi} = \hat{\boldsymbol{x}} - \boldsymbol{x}$, and $\beta^\delta = \int_{-\delta}^{\delta} \mu(|\boldsymbol{\xi}|)\, d\boldsymbol{\xi}$, $\hat{\mu}_k = \int_{-\delta}^{\delta} \mu(|\boldsymbol{\xi}|) \cos(k\boldsymbol{\xi})\, d\boldsymbol{\xi}$.

Therefore, as the separation constant Ψ^δ in Eq. (2.17) has been determined, the peridynamic analytical solution of the heat conduction equation can be concluded as follows [35]:

$$X(x) = \begin{cases} Gx + H, & \Psi^\delta = 0, \\ I \sin kx + J \cos kx, & \Psi^\delta \neq 0, \end{cases} \tag{2.18a}$$

$$T(t) = \begin{cases} E, & \Psi^\delta = 0, \\ Fe^{D\Psi^\delta t}, & \Psi^\delta \neq 0. \end{cases} \tag{2.18b}$$

Applying the boundary condition Eq. (2.4) to the peridynamic analytical Eq. (2.18), we get:

$$w(x, t; \tau) = \sum_{m=0}^{\infty} C_1 \sin k_m x \cdot \exp(D\Psi^\delta (t - \tau)), \tag{2.19}$$

where C_1 is the constant determined by the initial condition in Eq. (2.4). After applying the initial condition Eq. (2.4) to Eq. (2.19), this constant can be written as:

$$C_1 = \frac{2}{L}\int_0^L f(x,\tau)\sin k_m x\, dx, \tag{2.20}$$

where $f(x,\tau)$ is the external heat source at $t=\tau$. The last with the integral in Eq. (2.5) of Eq. (2.19), the peridynamic analytical solution for heat conduction with an external heat source can be expressed as:

$$\Theta(x,t) = \sum_{m=0}^{\infty}\int_0^t C_1 \sin k_m x \cdot \exp(D\Psi^{\delta}(t-\tau))d\tau. \tag{2.21}$$

Comparative analysis of Eq. (2.16b) and Eq. (2.18b), corresponding to the classical and peridynamic analytical solutions of heat conduction, respectively, demonstrates a fundamental distinction in their exponential function formulations. Therefore, the peridynamic factor or the nonlocal factor can be defined as [35]:

$$A_n(k,\delta) = \frac{\Psi^{\delta}}{\Psi^{c}}. \tag{2.22}$$

The introduction of a nonlocal factor enables explicit establishment of the relationship between classical and peridynamic analytical solutions for heat conduction problems, thereby facilitating quantitative assessment of nonlocal effects.

Therefore, the solution procedure involves two key steps: first transforming the inhomogeneous equation into its homogeneous form, then solving the resulting homogeneous integral equation within the peridynamic framework. This methodology ultimately yields the analytical solution for heat conduction problems incorporating an external heat source.

2.3. Nonlocal factor for one-dimensional peridynamic analytical solution

From the above study, we establish a fundamental connection between classical continuum mechanics and peridynamic analytical solutions for heat conduction problems through the introduction of a nonlocal factor. To obtain the expression of nonlocal factor, we choose the kernel function as [35]:

$$\mu(|\boldsymbol{\xi}|) = \begin{cases} \frac{3-n}{\delta^{3-n}}\frac{1}{|\boldsymbol{\xi}|^n}, & |\boldsymbol{\xi}| \le \delta, \\ 0, & |\boldsymbol{\xi}| > \delta, \end{cases} \qquad n = 0,1,2. \tag{2.23}$$

According to Eq. (2.17) and Eq. (2.23), a different value of n brings about different nonlocal factors. In detail, for $n = 0$ we have

$$A_0(r_m) = \frac{6\left[1 - \frac{\sin(r_m)}{r_m}\right]}{r_m^2}, \tag{2.24}$$

where $r_m = k_m\delta = \frac{m\pi}{L}\delta$ and $m = 1, 2, \ldots$. For $n = 1$, we have

$$A_1(r_m) = -\frac{4[\mathrm{Ci}(r_m) - \ln(r_m) - \gamma]}{r_m^2}, \tag{2.25}$$

where Ci is the cosine integral function with expression $\mathrm{Ci}(x) = \gamma + \ln(x) + \int_0^x \frac{\cos z - 1}{z}\, dz$; and γ is the Euler constant. For $n = 2$, we have

$$A_2(r_m) = \frac{2\left[\mathrm{Si}(r_m) + \frac{\cos(r_m)-1}{r_m}\right]}{r_m}, \tag{2.26}$$

where Si is the integral function and $\mathrm{Si}(x) = \int_0^x \frac{\sin z}{z}\, dz$.

2.4. Example 1: peridynamic analytical solution for one-dimensional insulation-dissipative heat conduction system

In this part, we discuss the peridynamic analytical solution for the one-dimensional insulation-dissipative heat conduction system. The governing equation is shown as Eq. (2.1); the boundary condition and initial condition are shown as Eq. (2.2) and Eq. (2.3), respectively.

We consider a special external heat source $f(x,t)$, for example, $f(x,t) = B\sin\omega t$. And the length of the finite one-dimensional domain is $L = 10$ cm, the diffusion coefficient $D = 1.14$ cm^2/s, the value of the amplitude and angular frequency is $B = 1^\circ$/s and $\omega = 1$ rad/s, respectively. Different from the homogeneous equation whose external source is zero, this nonzero external source introduces quite new different phenomena. Based on the method of separation of variables, the classical solution in Eqs. (2.1)–(2.3) is written as [37]:

$$\Theta(x,t) = \sum_{m=1}^{\infty} \frac{2B}{k_m L} \sin k_m x \frac{-D\Psi^c \sin\omega t - \omega\cos\omega t + \omega\exp(D\Psi^c t)}{\omega^2 + D^2(\Psi^c)^2}, \tag{2.27}$$

where Ψ^c is the separation constant and can be noted as:

$$\Psi^c = -k_m^2 = -\left(\frac{2m+1}{2}\frac{\pi}{L}\right)^2, \quad m = 1, 2, 3, \ldots. \tag{2.28}$$

Even though the governing equation is in different form for the classical and peridynamic heat conduction problem, the boundary conditions and initial

condition are the same. Based on Eq. (2.21), the peridynamic analytical solution can be written as:

$$\Theta(x,t)=\sum_{m=1}^{\infty}\frac{2B}{k_mL}\sin k_mx\frac{-D\Psi^{\delta}\sin\omega t-\omega\cos\omega t+\omega\exp(D\Psi^{\delta}t)}{\omega^2+D^2(\Psi^{\delta})^2}. \tag{2.29}$$

And according to the definition of the nonlocal factor in Eq. (2.22), the peridynamic analytical solution can be rewritten as:

$$\begin{aligned}\Theta_{pd}(x,t)&\\ =\sum_{m=1}^{\infty}\frac{2B}{k_mL}\sin k_mx&\frac{Dk_m^2A_n\sin\omega t-\omega\cos\omega t+\omega\exp(-Dk_m^2A_nt)}{\omega^2+D^2(-k_m^2A_n)^2}.\end{aligned} \tag{2.30}$$

A comparison between the solutions in Eq. (2.27) and Eq. (2.30) establishes a direct correspondence between classical and peridynamic heat conduction formulations. Specifically, the nonlocal factor A_n in the peridynamic solution appears precisely at locations corresponding to the separation constant Ψ^c in the classical solution. Unlike the heat conduction problem without the external heat source that the nonlocal factor A_n only appears at the exponential function [35], the heat conduction problem with an external heat source shows that the nonlocal factor not only appears at the exponential function but also appears at other places. The places where the nonlocal factor appears are determined by the position of the separation constant Ψ^c in the classical solution. This phenomenon originates fundamentally from the application of Duhamel's principle to problems involving the external heat source. The principle introduces integral terms into the solution formulation, thereby distributing the nonlocal factor A_n across multiple locations in the peridynamic solution. And the convergence and divergence analyze can be found in Appendix A. Besides, to our knowledge, there are currently no studies on peridynamic numerical solutions about heat conduction involving heat sources. Consequently, we are unable to compare the results of this paper with those from numerical calculations, and can only make comparisons with classical analytical solutions.

Figure 1 shows the peridynamic analytical solution of the one-dimensional insulation-dissipative heat conduction system with $t=(0.1,20,100,1000)$ s under the dimensionless horizon size $\delta/L=(0,0.05,0.1,0.2)$, and $n=2$ in the kernel function. The first 500 terms of the solution to peridynamic analytical series are chosen in Eq. (2.30). According to the conclusion in [35], $\delta/L=0$ represents the solution of classical continuum mechanics when the horizon size δ equals to zero. One can see that the dimensionless horizon size $\delta/L=0.2$ deviates the most from the classical solution, while $\delta/L=0.05$ deviates the least from the classical solution, showing good convergence of the horizon size, which

is consistent with the conclusion in [35]. And different from the heat conduction problem without an external heat source, the external source in this study will not only introduce the nonlocal factor in the exponential function but also in the remaining two other places in peridynamic analytical solution, which means that the nonlocal effect will keep working after a long time, as shown in Fig. 1d. This is a new phenomenon in heat conduction problems while an external heat source exists. It should also be noted that since the kernel function with $n = 2$ has the weakest nonlocal effect compared with $n = 0$ and $n = 1$ [35], the accuracy of the calculations with a larger dimensionless horizon size remains reliable. And next, we study the nonlocal effect based on the nonlocal factor aforementioned.

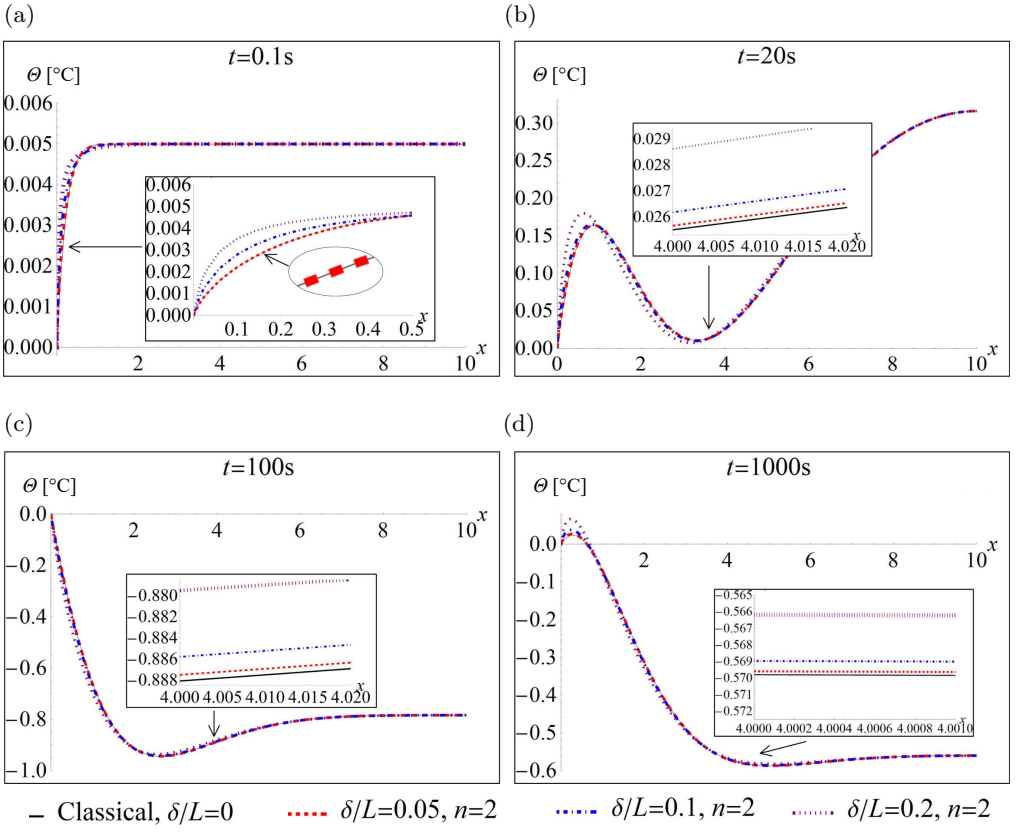

FIG. 1. One-dimensional insulation-dissipative heat conduction system with $t = (0.1, 20, 100, 1000)$ s under dimensionless horizon size $\delta/L = (0, 0.05, 0.1, 0.2)$, $n = 2$.

Figure 2 shows the peridynamic analytical solution of one-dimensional insulation-dissipative heat conduction system with $t = (0.3, 30, 60, 90)$ s under the horizon size $\delta/L = 0.1$, $n = 0, 1, 2$ in the kernel function. The first 20 000 terms of

peridynamic analytical series solution are chosen in Eq. (2.30). Since the applied external heat source $f(x,t)$ is a periodically varying function, the temperature distribution obtained from the peridynamic analytical solution is not monotonically varying. The non-smoothness of the curve near $x = 0$ can be improved by taking more terms in Eq. (2.30). We find that the kernel function with $n = 0$ shows the strongest nonlocal effect compared to the situations of $n = 1$ and $n = 2$ since it deviates more from the classical solution in Fig. 2, which is consistent with the findings in [35].

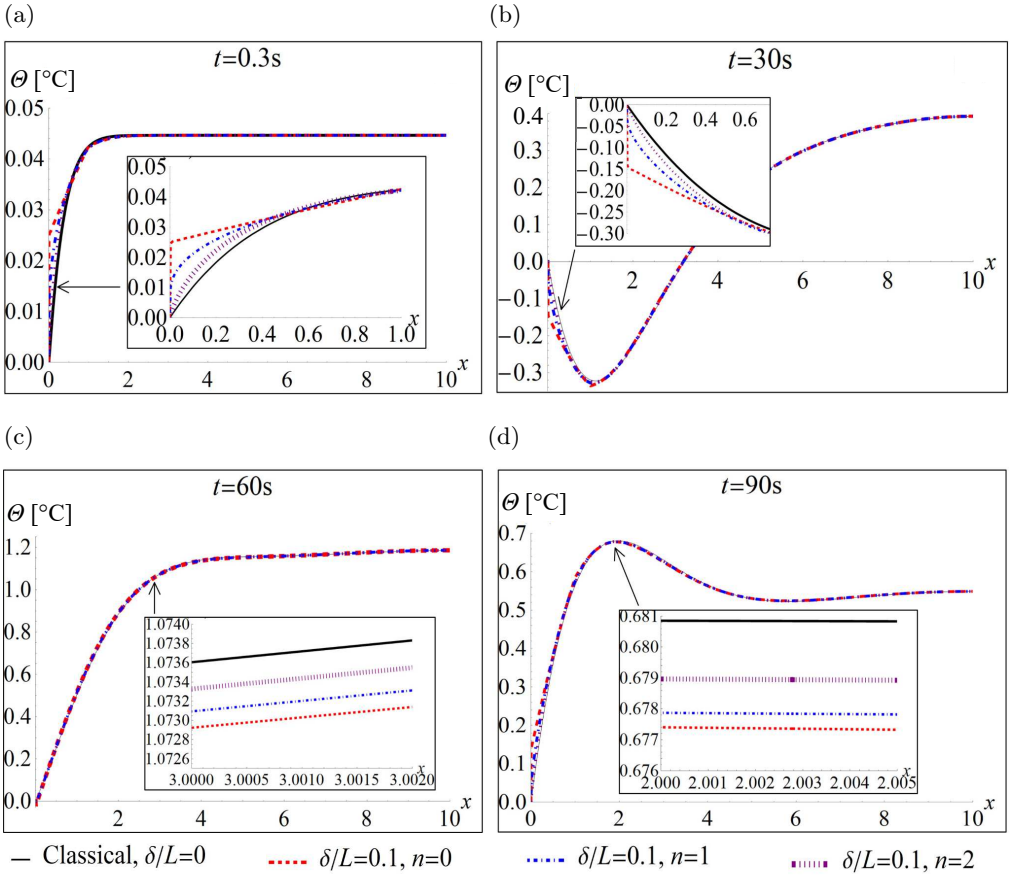

Fig. 2. One-dimensional insulation-dissipative system with $t = (0.3, 30, 60, 90)$ s under dimensionless horizon size $\delta/L = 0.1$, $n = 0, 1, 2$.

The preceding analysis demonstrates that while the inhomogeneous heat conduction equation with an external heat source can be transformed into an equivalent homogeneous form by incorporating the source effect into the initial conditions, the resulting temperature field exhibits non-monotonic temporal

evolution under continuous external heating. Furthermore, the presence of an external source fundamentally alters the structure of the peridynamic analytical solution compared to the source-free case. Specifically, the nonlocal factor A_n appears not only in the exponential terms but also in additional components of the solution, leading to a significantly slower decay of nonlocal effects.

While the analytical solutions are expressed as series expansions rather than closed-form expressions, their computational implementation differs fundamentally from numerical methods. The series terms are computed through direct summation of analytical expressions, eliminating the need for spatial discretization, iterative solvers, or numerical quadrature. This analytical approach maintains well-controlled computational costs while achieving superior efficiency compared to conventional numerical techniques.

Table 1 presents the computational time required for evaluating Eq. (2.29) (classical solution), Eq. (2.30) (peridynamic analytical solution) under standard hardware conditions (Intel(R) Core(TM) i7-14700KF 3.40 GHz) with varying numbers of series terms. The results demonstrate a near-linear scaling of computation time with respect to the number of terms, reflecting the absence of iterative overhead characteristic of numerical methods. Notably, the total computational expenditure remains consistently lower than conventional numerical simulations for equivalent problem configurations.

TABLE 1. The computation time used for the classical solution (Eq. (2.29)) and the peridynamic analytical solution (Eq. (2.30)) when different numbers of terms are taken.

Terms	Computation time (Eq. (2.29))	Computation time (Eq. (2.30))
500	0.008 s	0.063 s
1000	0.017 s	0.106 s
2000	0.020 s	0.150 s

3. Analytical solution for two-dimensional nonlocal heat conduction with an external heat source in a finite rectangle domain

In this section we study the two-dimensional peridynamic analytical solution for heat conduction with an external heat source in a finite rectangle domain. The inhomogeneous heat conduction equation, boundary condition, and initial condition in two-dimension are:

$$
\begin{cases}
\frac{\partial \Theta}{\partial t} = D\big(\frac{\partial^2 \Theta}{\partial x^2} + \frac{\partial^2 \Theta}{\partial y^2}\big) + f(x,y,t), & 0 < x < L, t > 0, \\
\Theta(0,y,t) = 0,\ \Theta(L,y,t) = 0, & t > 0, \\
\Theta(x,0,t) = 0,\ \Theta(x,H,t) = 0, & t > 0, \\
\Theta(x,y,0) = 0, & 0 < x < L,
\end{cases}
\tag{3.1}
$$

where $f(x,y,t)$ is the external heat source; H and L are the width and length of the rectangle domain. As it is done in the one-dimensional problem, applying Duhamel's principle to Eq. (3.1) transforms this inhomogeneous equation into a homogeneous equation, and the effect of the external source will transfer into the initial condition, namely:

$$\begin{cases} v_t = D(v_{xx} + v_{xy}), & 0 < x < L, t > \tau, \\ v(0,y,t) = 0,\ v(L,y,t) = 0, & t > \tau, \\ v(x,0,t) = 0,\ v(x,H,t) = 0, & t > \tau, \\ v(x,y,\tau) = f(x,y,\tau), & 0 < x < L, t > \tau, \end{cases} \tag{3.2}$$

where the function v satisfies

$$\Theta(x,y,t) = \int_0^t v(x,y,t;\tau)\,d\tau. \tag{3.3}$$

To verify the equivalence of the governing equation, Eq. (3.3) is derived and the results are substituted into Eq. $(3.1)_1$, resulting in

$$\begin{aligned} &\frac{\partial\Theta}{\partial t} - D\left(\frac{\partial^2\Theta}{\partial x^2} + \frac{\partial^2\Theta}{\partial y^2}\right) \\ &= \int_0^t \frac{\partial v(x,y,t;\tau)}{\partial t}\,d\tau + v(x,y,t;\tau)|_{\tau=t} - D\int_0^t \left(\frac{\partial^2 v(x,y,t;\tau)}{\partial x^2} + \frac{\partial^2 v(x,y,t;\tau)}{\partial y^2}\right) d\tau \\ &= f(x,y,t), \end{aligned} \tag{3.4}$$

which means that Eq. (3.3) is the solution of Eq. $(3.1)_1$.

To verify the boundary condition, we have:

$$\begin{aligned} \Theta(0,y,t) &= \int_0^t v(x,y,t;\tau)|_{x=0}\,d\tau = 0, \\ \Theta(L,y,t) &= \int_0^t v(x,y,t;\tau)|_{x=L}\,d\tau = 0, \\ \Theta(x,0,t) &= \int_0^t v(x,y,t;\tau)|_{y=0}\,d\tau = 0, \\ \Theta(x,H,t) &= \int_0^t v(x,y,t;\tau)|_{y=H}\,d\tau = 0. \end{aligned} \tag{3.5}$$

Finally, as far as the initial conditions are concerned, we have

$$\Theta(x,y,0) = \int_0^{t=0} v(x,y,t;\tau)\,d\tau = 0. \tag{3.6}$$

So far, Eqs. (3.4)–(3.6) have verified the equivalence between Eq. (3.1) and Eq. (3.2) by the tackle of the Duhamel's principle, and its analytical peridynamic solution can be obtained based on the classical solution.

3.1. Peridynamic analytical solution for two-dimensional heat conduction with an external heat source in a finite rectangle domain

When solving Eq. (3.2), one should note that the time does not start from $t = 0$ but from $t = \tau$. This can be dealt with the mathematical transformation $t' = t - \tau$. The heat conduction equation corresponding to Eq. (3.2) about time t' in peridynamics is:

$$\begin{cases} \frac{\partial V}{\partial t'} = DL_\delta V(x,t'), & 0 < x < L,\ t' > 0, \\ V(0,y,t') = 0,\ V(L,y,t') = 0, & t' > 0, \\ V(x,0,t') = 0,\ V(x,H,t') = 0, & t' > 0, \\ V(x,y,0) = f(x,y,\tau), & 0 < x < L,\ t' > 0, \end{cases} \tag{3.7}$$

where the peridynamic Laplacian operator can be written as

$$L_\delta V(\boldsymbol{x},t') = \int_{H_{\boldsymbol{x}}} \mu(|\hat{x} - \boldsymbol{x}|)[V(\hat{x},t') - V(\boldsymbol{x},t')]\,dV_{\hat{\boldsymbol{x}}}. \tag{3.8}$$

According to the method of separation of variables, let $V(x,y,t') = S(x,y)T(t')$, yielding

$$\frac{L_\delta S(x,y)}{S(x,y)} = \frac{1}{D}\frac{T'(t')}{T(t')} = \Psi^\delta, \tag{3.9}$$

where Ψ^δ is the separation constant related to the nonlocal factor. We may find the solution of integral equation in Eq. (3.9) by sticking to the classical homogeneous heat conduction equation

$$\frac{\partial V}{\partial t'} = D\left(\frac{\partial^2 V}{\partial x^2} + \frac{\partial^2 V}{\partial y^2}\right) \tag{3.10}$$

and let $S(x,y) = X(x)Y(y)$, one can get the classical solution as:

$$\begin{cases} X(x) = C_1\cos(\sqrt{\lambda_1}x) + C_2\sin(\sqrt{\lambda_1}x), \\ Y(x) = C_3\cos(\sqrt{\lambda_2}y) + C_4\sin(\sqrt{\lambda_2}y). \end{cases} \tag{3.11}$$

When we assume that Eq. (3.11) satisfies the integral equation in Eq. (3.9), one can obtain the nonlocal factor A_n. The details about nonlocal factor can be found in Section 3.2. Using the boundary conduction and initial condition in Eq. (3.7), and solving the ordinary differential equation about time t' in Eq. (3.9), one can obtain the solution of Eq. (3.7) as

$$V(x,y,t') = \sum_{n_1=0}^{\infty}\sum_{m_1=0}^{\infty}\frac{4}{LH}\int_0^H\int_0^L f(x,y,\tau)\sin\frac{n_1\pi}{L}x\cdot\sin\frac{m_1\pi}{H}y\,dx\,dy \cdot\sin\frac{n_1\pi}{L}x\cdot\sin\frac{m_1\pi}{H}y\cdot\exp(D\Psi^{\delta}t'), \tag{3.12}$$

where the separation constant Ψ^{δ} can be determined based on the nonlocal factor A_n. Thus the heat conduction problem with an external source is

$$\begin{aligned}\Theta(x,y,t) &= \int_0^t V(x,y,t';\tau)\,d\tau \\ &= \int_0^t \sum_{n_1=0}^{\infty}\sum_{m_1=0}^{\infty} C_{m_1n_1}\sin\frac{n_1\pi}{L}x\sin\frac{m_1\pi}{H}x\cdot\exp(D\Psi^{\delta}(t-\tau))\,d\tau,\end{aligned} \tag{3.13}$$

where

$$C_{m_1n_1} = \frac{4}{LH}\int_0^H\int_0^L f(x,y,\tau)\sin\frac{n_1\pi}{L}x\cdot\sin\frac{m_1\pi}{H}y\,dx\,dy. \tag{3.14}$$

3.2. Nonlocal factor for two-dimensional peridynamic analytical solution

Using the similar derivation as it is done in Section 2.2, we assume that the classical solution about space x and y can satisfy the peridynamic integral equation, and then deriving the two-dimensional nonlocal factor as [35]:

$$A_n(k_1,k_2,\delta) = \frac{\Psi^{\delta}}{\Psi^{c}} = \frac{2\pi\hat{\mu}_k-\beta^{\delta}}{-(k_1^2+k_2^2)} = -2\pi\frac{\delta^4}{r^4}\int_0^r \mu\left(\frac{\delta R}{r}\right)R[J_0(R)-1]\,dR, \tag{3.15}$$

where $J_0(R)$ is the zero-order Bessel function of the first kind; $k_1 = n_1\pi/L$, $k_2 = m_1\pi/L$. And the detail of derivation of the nonlocal factor can be found in [35].

The kernel function is chosen as:

$$\mu(|\boldsymbol{\xi}|) = \begin{cases}\frac{2(4-n)}{\pi\delta^{4-n}}\frac{1}{|\boldsymbol{\xi}|^n}, & |\boldsymbol{\xi}|\le\delta,\\ 0, & |\boldsymbol{\xi}|\ge\delta,\end{cases} \quad n=0,1,2,\ldots. \tag{3.16}$$

Substituting Eq. (3.16) into Eq. (3.15), one obtains the nonlocal factor as

$$A_n(k_{m_1}, k_{n_1}, \delta) = -\frac{4(4-n)}{r^{4-n}} \int_0^r \frac{J_0(R)-1}{R^{n-1}}\, dR, \tag{3.17}$$

where $r = \sqrt{(k_{m_1}\delta)^2 + (k_{n_1}\delta)^2}$ and $k_{m_1} = \frac{m_1\pi}{H}$, $k_{n_1} = \frac{n_1\pi}{L}$.

When the integral in Eq. (3.17) is calculated, the nonlocal factor can be further expressed in the hypergeometric function ${}_aF_b$ as:

$$A_n(k_{m_1}, k_{n_1}, \delta) = A_n(r) = \begin{cases} \frac{8}{r^3}(r - 2J_1(r)), & n = 0, \\ \frac{12}{r^2}\big(1 - {}_1F_2\big(\frac{1}{2}; 1, \frac{3}{2}; -\frac{r^2}{4}\big)\big), & n = 1, \\ {}_2F_2\big(1, 1; 2, 2, 2; -\frac{r^2}{4}\big), & n = 2, \end{cases} \tag{3.18}$$

where J_1 is the Bessel function of the first-order.

3.3. Example 2: peridynamic analytical solution for two-dimensional heat conduction

Consider the constant external heat source $f(x, y, t) = 100°/\text{s}$. The size of the rectangle is $H = L = 10$ cm, the diffusion coefficient $D = 1.14$ cm^2/s.

The classical solution with the same external source can be obtained with the method of separation of variables as

$$\Theta(x, y, t) = \sum_{n_1=1,3,5,\ldots}^{\infty} \sum_{m_1=1,3,5,\ldots}^{\infty} \frac{\frac{16T_0}{m_1 n_1 \pi^2} \cdot \sin\frac{n_1\pi}{L}x \cdot \sin\frac{m_1\pi}{H}y}{-\Psi^c D}[1 - \exp(\Psi^c D t)]. \tag{3.19}$$

According to Eq. (3.13) and the definition of the nonlocal factor in Eq. (3.15), the peridynamic analytical solution with a constant external source $f(x, y, t) = 100°/\text{s}$ can be written as

$$\Theta_{pd}(x, y, t) = \sum_{n_1=1,3,5,\ldots}^{\infty} \sum_{m_1=1,3,5,\ldots}^{\infty} \frac{\frac{16T_0}{m_1 n_1 \pi^2} \cdot \sin\frac{n_1\pi}{L}x \cdot \sin\frac{m_1\pi}{H}y}{-A_n(k_m, k_n, \delta)\Psi^c D} \times [1 - \exp(A_n(k_m, k_n, \delta)\Psi^c D t)], \tag{3.20}$$

where $T_0 = 100$ is a constant external heat source. The convergence of this series solution can be found in [35].

Comparative analysis of the peridynamic (Eq. (3.20)) and classical (Eq. (3.19)) heat conduction solutions with an external source reveals that the peridynamic analytical solution is obtained through substitution of the separation constant Ψ^c

in the classical solution with the modified term $A_n\Psi^c$ [35]. The application of Duhamel's principle introduces integral terms into the solution, resulting in the nonlocal factor A_n appearing not only in the exponential function but also in other components of the peridynamic solution. Consequently, unlike source-free cases where nonlocal effects diminish over time, the external heat source maintains the influence of the nonlocal factor indefinitely, leading to persistent nonlocal effects as time t goes to infinity.

Figure 3 shows the two-dimensional peridynamic analytical solution at different time t and n with a certain dimensionless horizon size $\delta/L = 0.4$. The first 90 000 terms of peridynamic analytical series solution are chosen in Eq. (3.20). Since the peridynamic analytical solution is symmetric about the x- and y-axes, we only show half temperature distribution of the result in y-axes, namely $y \in [0, 5]$. In contrast to the homogeneous case without the external heat source, the inhomogeneous equation exhibits monotonically increasing temperature evolution. To quantitatively assess the external source's influence, we evaluate the temperature field Θ at the rectangular plate's centroid ($x = y = 5$ cm), with Fig. 3 explicitly marking this location (black dot) and displaying its value. Comparative analysis reveals that the peridynamic solution demonstrates stronger agreement with classical continuum mechanics when using $n = 2$ in the kernel function, while greater deviation occurs for $n = 0$ at equivalent time instances.

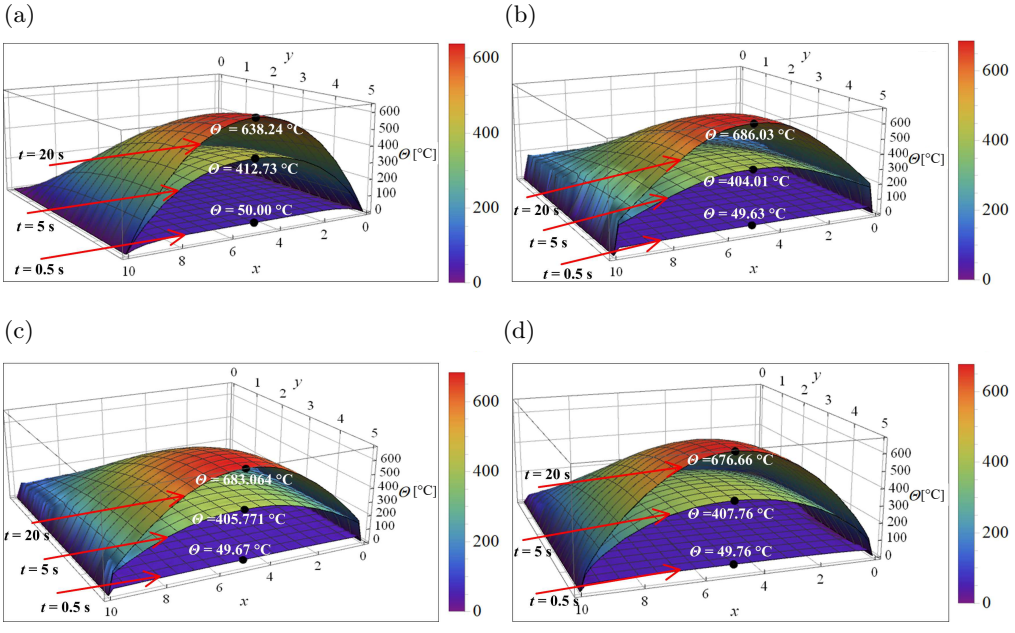

Fig. 3. Two-dimensional peridynamic analytical solution at $t = (0.5, 5, 20)$ s. (a) Classic solution; peridynamic analytical solution with $\delta/L = 0.4$ and (b) $n = 0$; (c) $n = 1$; (d) $n = 2$.

This systematic variation conclusively demonstrates that the kernel parameter n governs nonlocal effects, with $n = 0$ producing the strongest nonlocality and $n = 2$ yielding the weakest nonlocal behavior.

To further show the difference between the classical analytical solution and the peridynamic one, we exhibit their difference value $\Delta\Theta$ (classical solution minus peridynamic solution) in Fig. 4. The same as it is in Fig. 3, the first 90 000 terms in Eq. (3.20) are chosen. The reasons for selecting the number of terms can be found in Appendix B. Equation (3.20) demonstrates that the peridynamic analytical solution comprises a superposition of sinusoidal functions in both x and y directions, with the maximum temperature Θ occurring

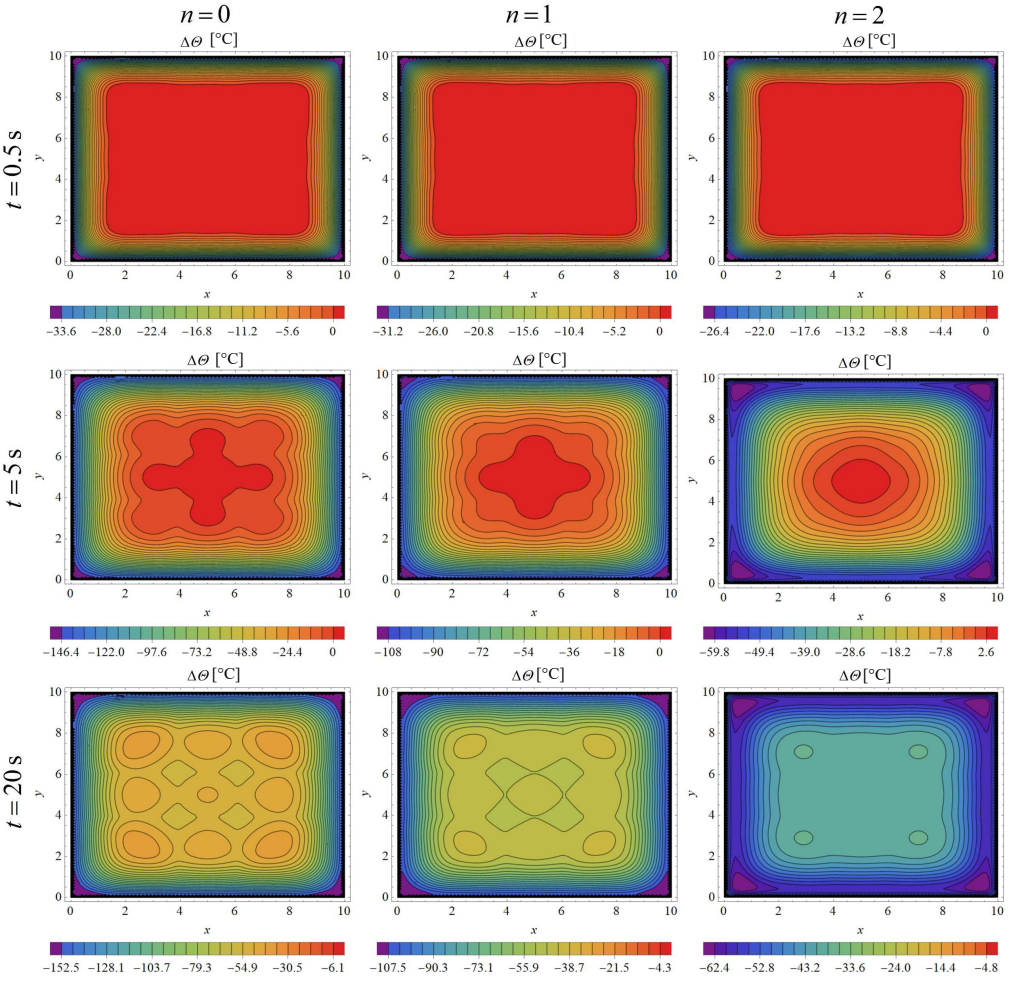

FIG. 4. The difference value $\Delta\Theta$ between the classical solution and peridynamic analytical solution. Peridynamic analytical solution with $\delta/L = 0.4$ and $n = 0, 1, 2$.

at the rectangular plate's centroid. As illustrated in Fig. 3, the temperature field exhibits radial symmetry, decaying monotonically from the centroid along all spatial directions. On the other hand, the peridynamic analytical solution in Eq. (3.20) is also related to the function f_1 and the nonlocal factor function f_2, which are noted as:

$$f_1 = 1 - \exp(A_n \Psi^c D t), \qquad f_2 = \frac{1}{A_n}. \tag{3.21}$$

During the process of heat conduction, both the exponential function f_1 and the nonlocal factor function f_2 will affect the temperature distribution in peridynamics. In detail, compared to the classical solution, the exponential function f_1 will shrink the peridynamic analytical solution while f_2 will expand it since the value of the nonlocal factor A_n is between 0 and 1. At shorter timescales ($t = 0.5$ s and $t = 5$ s), the dominant contribution from f_2 relative to f_1 results in enhanced temperature values in the peridynamic solution. This effect, combined with the spatial sinusoidal distribution in x and y directions, leads to more pronounced difference between classical and peridynamic solutions near the boundaries compared to the central region, as evidenced in the first two rows of Fig. 4. At extended timescales ($t = 20$ s), the diminishing influence of f_1 and predominant contribution from f_2 cause the peridynamic solution to consistently exceed the classical solution, accounting for the negative temperature differences shown in the third row of Fig. 4. The analysis further reveals that the spatial domain where the classical solution exceeds the peridynamic solution progressively diminishes with increasing time, ultimately vanishing completely. Moreover, comparative evaluation of kernel function parameters demonstrates systematically stronger temperature fields for $n = 0$ relative to $n = 2$, reconfirming that $n = 0$ produces the most pronounced nonlocal effects while $n = 2$ yields the weakest nonlocal behavior in the solution. Since the temperature distribution $\Delta\Theta$ is calculated with a rough dimensionless horizon size $\delta/L = 0.4$, the results of the calculations are not very regular, which inspires us to investigate the convergence of the horizon size in the following research.

Figure 5 shows the convergence of the dimensionless horizon δ/L with respect to the difference value $\Delta\Theta$ between the classical analytical solution and the peridynamic one when $n = 2$ in the kernel function. In order to balance the smoothness of the image and computational efficiency, the first 160 000 terms Eq. (3.20) are chosen. The reasons for selecting the number of terms can be found in Appendix B. The analysis reveals that decreasing the dimensionless horizon size δ/L leads to a corresponding reduction in the temperature distribution difference $\Delta\Theta$, demonstrating the convergence characteristics of the horizon size parameter. Consistent with the behavior shown in Fig. 4, the temperature difference $\Delta\Theta$ exhibits larger values in boundary regions compared to the central

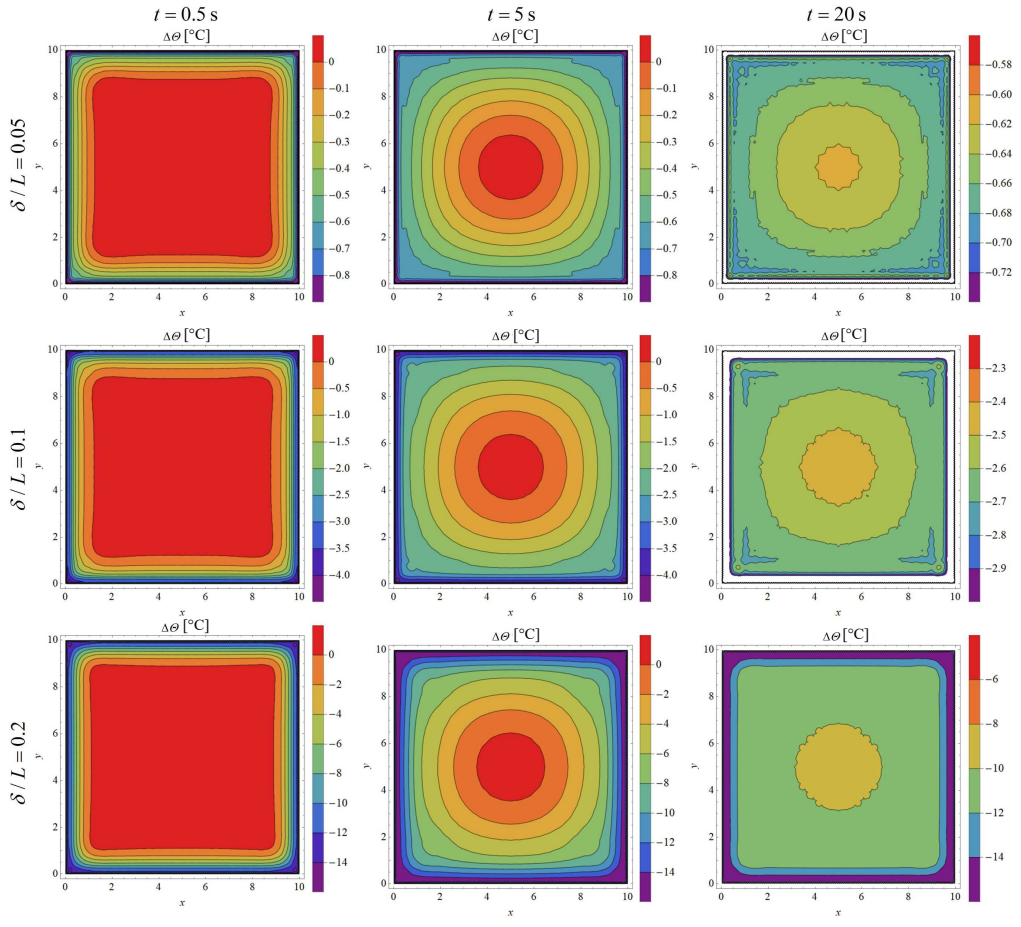

FIG. 5. The effect of dimensionless horizon size δ/L on $\Delta\Theta$ when $n = 2$, $t = (0.5, 5, 20)$ s.

area during initial time periods. Furthermore, as time progresses toward infinity, the temperature difference maintains negative values throughout the entire rectangular domain.

Similar to the one-dimensional case, this analytical approach maintains well-controlled computational costs while achieving superior efficiency compared to conventional numerical techniques. Taking the situation at $\delta/L = 0.1$, $n = 2$, $t = 5$ s as an example, Table 2 reveals the computational time scaling with both term count and solution accuracy. As evidenced in Table 2, computational time increases progressively with the number of series terms, indicating that higher solution accuracy requires proportionally greater computational resources.

The finite element analysis of temperature fields necessitates iterative computations at each time step, leading to cumulative increases in computational

Table 2. The computation time used for the classical solution (Eq. (3.19)) and the peridynamic analytical solution (Eq. (3.20)) when different numbers of terms are taken. $\delta/L = 0.1$, $n = 2$, $t = 5$ s.

Terms	Computation time (Eq. (3.19))	Computation time (Eq. (3.20))
40 000 ($n_1 = 200$, $m_1 = 200$)	0.135 s	15.825 s
90 000 ($n_1 = 300$, $m_1 = 300$)	0.296 s	43.258 s
160 000 ($n_1 = 400$, $m_1 = 400$)	0.526 s	91.580 s

demand with increasing simulation time. In contrast, the analytical approach maintains constant computational requirements regardless of temporal progression, as evidenced by the consistent resource utilization shown in Table 2 for solutions at $t = 5$ s and Table 3 for solutions at $t = 200$ s, respectively. Quantitative comparisons in Table 3 demonstrate that the computation time for various term counts at $t = 200$ s remains equivalent to that at $t = 5$ s (Table 2), establishing the inherent efficiency advantage of our methodology over conventional finite element approaches.

Table 3. The computation time used for the classical solution (Eq. (3.19)) and the peridynamic analytical solution (Eq. (3.20)) when different numbers of terms are taken. $\delta/L = 0.1$, $n = 2$, $t = 200$ s.

Terms	Computation time (Eq. (3.19))	Computation time (Eq. (3.20))
40 000 ($n_1 = 200$, $m_1 = 200$)	0.139 s	16.096 s
90 000 ($n_1 = 300$, $m_1 = 300$)	0.297 s	43.811 s
160 000 ($n_1 = 400$, $m_1 = 400$)	0.529 s	93.291 s

4. Conclusion

This work presents analytical peridynamic solutions for one- and two-dimensional heat conduction problems incorporating an external heat source. Through application of Duhamel's principle, the inhomogeneous governing equation with an external source term is transformed into an equivalent homogeneous form, enabling solution via separation of variables. The introduction of a nonlocal factor establishes a fundamental connection between classical continuum mechanics and peridynamic solutions, thereby facilitating direct derivation of the peridynamic analytical solution from its classical counterpart.

The present study reveals fundamental differences between peridynamic systems with and without the external heat source. For both one- and two-dimen-

sional heat conduction problems involving the external source, the nonlocal factor appears not only in exponential terms but also in other components of the peridynamic analytical solution. This phenomenon results in persistent nonlocal effects that maintain their influence as time approaches infinity. Specifically, in the one-dimensional case with a sinusoidal external heat source, the temperature field demonstrates continuous temporal evolution without attenuation. The investigation of two-dimensional heat conduction under an external heat source reveals that the nonlocal factor exhibits dual modulation of the peridynamic solution through attenuate behavior in exponential terms and incremental characteristics in non-exponential components, leading to distinct temperature distribution patterns. These findings, consistently observed in both dimensional analyses, demonstrate that the kernel function with a parameter $n = 0$ induces the strongest nonlocal effects while $n = 2$ corresponds to the weakest localized response. Furthermore, this finding demonstrates the enhanced computational efficiency of the proposed methodology in comparison to conventional finite element calculations. The developed methodology establishes a novel approach for deriving peridynamic analytical solutions to externally-driven heat conduction problems, significantly advancing the application scope of peridynamic theory in thermal analysis.

The derivation of three-dimensional analytical solutions follows a similar methodology to the two-dimensional case, although with substantially increased mathematical complexity, particularly regarding convergence verification of the series expansions. To establish rigorous foundations for our current 2D analysis, we strategically prioritized comprehensive validation in the lower-dimensional space before proceeding to 3D extensions. This systematic approach ensures methodological robustness while providing essential groundwork for our ongoing investigations into the full three-dimensional formulation.

Appendix A. Proof of the convergence of peridynamic solution

This appendix discusses the convergence of the peridynamic solution. For the series solution in the one-dimensional example shown in Eq. (2.30), we have

$$\Theta_{pd}(x,t) = \sum_{m=1}^{\infty} u_m, \tag{A1}$$

where

$$\Theta_m = \frac{2B}{k_m L} \sin k_m x \frac{Dk_m^2 A_n \sin \omega t - \omega \cos \omega t + \omega \exp(-Dk_m^2 A_n t)}{\omega^2 + D^2(-k_m^2 A_n)^2}.$$

For $n = 2$, the cosine function terms in the nonlocal factor $A_2(r_m)$ approaches to zero as m approaches infinity, namely

$$\lim_{m\to+\infty}\frac{\cos(r_m)-1}{r_m}=\lim_{m\to+\infty}\frac{\cos\left(\frac{m\pi}{L}\delta\right)-1}{\frac{m\pi}{L}\delta}=0. \tag{A2}$$

Thus the limitation of $k_m^2 A_2$ can be calculated as:

$$\begin{aligned}\lim_{m\to+\infty}k_m^2A_2&=\lim_{m\to+\infty}k_m^2\frac{2\left[\mathrm{Si}(r_m)+\frac{\cos(r_m)-1}{r_m}\right]}{r_m}\\&=\lim_{m\to+\infty}\frac{2m\pi}{L\delta}\left[\mathrm{Si}\left(\frac{m\pi}{L}\delta\right)+\frac{\cos(r_m)-1}{r_m}\right]\\&=\lim_{m\to+\infty}\frac{2m\pi}{L\delta}\mathrm{Si}\left(\frac{m\pi}{L}\delta\right)=\frac{m\pi^2}{L\delta}.\end{aligned} \tag{A3}$$

In the above derivation $\mathrm{Si}(+\infty)=\frac{\pi}{2}$ is used.

To study the convergence of the series solution, the method of scaling and p-series are used. Due to that $|\sin k_m x|\le 1$, $|\sin\omega t|\le 1$, $|\cos\omega t|\le 1$, scaling Eq. (A1) leads to

$$\begin{aligned}|\Theta_n|&\le\frac{2B}{k_mL}\frac{Dk_m^2A_n+|\omega|+|\omega|}{\omega^2+D^2(-k_m^2A_n)^2}\le\frac{2B}{k_mL}\frac{Dk_m^2A_n}{\omega^2+D^2(-k_m^2A_n)^2}\\&=C_4\frac{1}{m^2+C_3},\end{aligned} \tag{A4}$$

where

$$C_3=\frac{L^2\omega^2\delta^2}{D^2\pi^4},\qquad C_4=\frac{2BL\delta}{D^2\pi^3}.$$

Due to that $\frac{1}{m^2+C_3}$ and $\frac{1}{m^2}$ show similar trends of change, they have the same convergence and divergence. We know that $\sum_{m=1}^{\infty}\frac{1}{m^2}$ is p-series with $p=2$, and $p>1$ means the series $\sum_{m=1}^{\infty}\frac{1}{m^2}$ converges. That is to say series $\sum_{m=1}^{\infty}C_4\frac{1}{m^2+C_3}$ also converges. Based on the comparison test for convergence, it can be concluded that the series $\sum_{m=1}^{\infty}|\Theta_m|$ converges, specifically, absolutely converges. From the relationship of absolute convergence and convergence, we can say that the series $\sum_{m=1}^{\infty}\Theta_m$ converges, namely the peridynamic solution in Eq. (A1) or Eq. (2.30) converges.

For $n=0$ and $n=1$, the scaling method fails, and their convergence remains to be further investigated in the future.

Appendix B. Basis for selecting the number of series terms in 2D calculations

The determination of 90 000 and 160 000 terms in the 2D simulations was established through systematic convergence analysis, where we incrementally in-

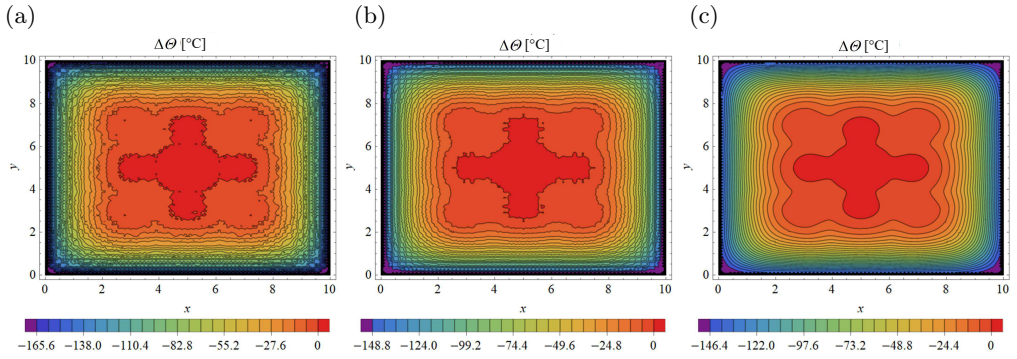

FIG. 6. The difference value $\Delta\Theta$ between the classical solution and peridynamic analytical solution with $\delta/L = 0.4$, $n = 0$ and $t = 5$ s. (a) The first 10 000 terms ($n_1 = 100$ and $m_1 = 100$); (b) The first 40 000 terms ($n_1 = 200$ and $m_1 = 200$); (c) The first 90 000 terms ($n_1 = 300$ and $m_1 = 300$).

creased the term count until achieving solution stability within acceptable tolerance limits. This rigorous approach ensures numerical reliability while optimizing computational efficiency.

Taking the situation at $n = 0$ and $t = 5$ s as an example, we explain the basis for selecting the first 90 000 ($n_1 = 300$ and $m_1 = 300$) terms of the series. Figure 6 illustrates the evolving difference between classical and peridynamic solutions at $\delta/L = 0.4$, clearly demonstrating the progressive convergence of the peridynamic solution with increasing term counts. This convergence behavior motivated our selection of 90 000 terms for generating Fig. 4.

Taking the situation at $t = 5$ s as an example, we explain the basis for selecting the first 160 000 terms of the series in Fig. 5. Figure 7 shows the effect

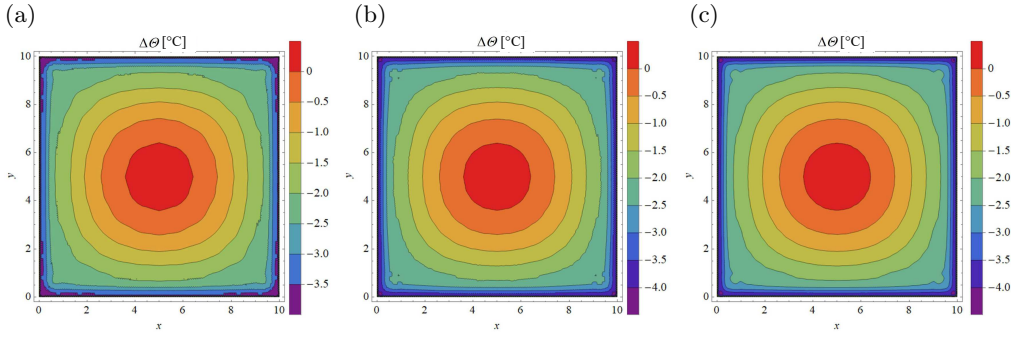

FIG. 7. The effect of dimensionless horizon $\delta/L = 0.1$ on $\Delta\Theta$ when $n = 2$, $t = 5$ s. (a) The first 40 000 terms ($n_1 = 200$ and $m_1 = 200$); (b) The first 90 000 terms ($n_1 = 300$ and $m_1 = 300$); (c) The first 160 000 terms ($n_1 = 400$ and $m_1 = 400$).

of the dimensionless horizon δ/L on $\Delta\Theta$ when $n = 2$. In the calculation, the first 160 000 terms are taken in Eq. (3.20), i.e., $n_1 = 400$ and $m_1 = 400$. It can be seen from Fig. 7 that as the number of terms in the series solution increases, the difference between the peridynamic analytical solution and the classical solution gradually stabilizes, and the peridynamic analytical solution gradually converges. Based on the convergence analysis, we use the first 160 000 terms for the analysis in Fig. 5.

Acknowledgements

This research is funded by the Fundamental Research Funds for the Central Universities, Jinan University (Grant No. 21624332); Youth Innovation Talent Project of General Higher Education Institutions in Guangdong Province (2024KQNCX007); Basic Research Program of Guangzhou Municipal Science and Technology Bureau (2025A04J3809). We would like to thank Professor Ziguang Chen in Huazhong University of Science and Technology for his guidance and advice. We would also like to thank Professor Heng Xiao, associate professor Zhihua Ning, Lin Zhan and lecturer Siyu Wang in Jinan University for their help during the research.

References

1. E. Kröner, *Elasticity theory of materials with long range cohesive forces*, International Journal of Solids and Structures, **3**, 731–742, 1967, https://doi.org/10.1016/0020-7683(67)90049-2.

2. A.C. Eringen, *Linear theory of nonlocal elasticity and dispersion of plane waves*, International Journal of Engineering Science, **10**, 425–435, 1972, https://doi.org/10.1016/0020-7225(72)90050-X.

3. A.C. Eringen, D.G.B. Edelen, *On nonlocal elasticity*, International Journal of Engineering Science, **10**, 233–248, 1972, https://doi.org/10.1016/0020-7225(72)90039-0.

4. I.A. Kunin, *Inhomogeneous elastic medium with nonlocal interaction*, Journal of Applied Mechanics and Technical Physics, **8**, 41–44, 1967, https://doi.org/10.1007/BF00913207.

5. S.A. Silling, *Reformulation of elasticity theory for discontinuities and long-range forces*, Journal of the Mechanics and Physics of Solids, **48**, 175–209, 2000, https://doi.org/10.1016/S0022-5096(99)00029-0.

6. O. Weckner, R. Abeyaratne, *The effect of long-range forces on the dynamics of a bar,* Journal of the Mechanics and Physics of Solids, **53**, 705–728, 2005, https://doi.org/10.1016/j.jmps.2004.08.006.

7. J.M. Zhang, M. Yu, X.H. Chu, *Coupled hygro-thermo-mechanical peridynamic model for concrete fracture analysis at high temperature*, Computational Particle Mechanics, **11**, 1661–1680, 2023, https://doi.org/10.1007/s40571-023-00695-7.

8. Z.B. Li, F. Han, *Adaptive coupling of non-ordinary state-based peridynamics and classical continuum mechanics for fracture analysis*, Computer Methods in Applied Mechanics and Engineering, **420**, 116691, 2024, https://doi.org/10.1016/j.cma.2023.116691.

9. K. Feng, X.P. Zhou, *Peridynamic simulation of the mechanical responses and fracturing behaviors of granite subjected to uniaxial compression based on CT heterogeneous data*, Engineering with Computers, **39**, 307–329, 2023, https://doi.org/10.1007/s00366-021-01549-7.

10. X. Gu, X. Li, X.Z. Xia, E. Madenci, Q. Zhang, *A robust peridynamic computational framework for predicting mechanical properties of porous quasi-brittle materials*, Composite Structures, **303**, 116245, 2023, https://doi.org/10.1016/j.compstruct.2022.116245.

11. M. Yu, Z.Y. Zhou, Z.X. Huang, *Traction-associated peridynamic motion equation and its verification in the plane stress and fracture problems*, Materials, **16**, 2252, 2023, https://doi.org/10.3390/ma16062252.

12. J. Zhang, Y.X. Liu, X. Lat, L.S. Liu, H. Met, X. Liu, *A modified bond-associated non-ordinary state-based peridynamic model for impact problems of quasi-brittle materials*, Materials, **16**, 4050, 2023, https://doi.org/10.3390/ma16114050.

13. B.F. Chu, Q.W. Liu, L.S. Liu, X. Lat, H. Mei, *A rate-dependent peridynamic model for the dynamic behavior of ceramic materials*, Computer Modeling in Engineering & Sciences, **124**, 151–178, 2020, https://doi.org/10.32604/cmes.2020.010115.

14. L.W. Wu, D. Huang, *Peridynamic modeling and simulations on concrete dynamic failure and penetration subjected to impact loadings*, Engineering Fracture Mechanics, **259**, 108135, 2022, https://doi.org/10.1016/j.engfracmech.2021.108135.

15. S. Jafarzadeh, J.M. Zhao, M. Shakouri, F. Bobaru, *A peridynamic model for crevice corrosion damage*, Electrochimica Acta, **401**, 139512, 2022, https://doi.org/10.1016/j.electacta.2021.139512.

16. Z.G. Chen, S. Jafarzadeh, J.M. Zhao, F. Bobaru, *A coupled mechano-chemical peridynamic model for pit-to-crack transition in stress-corrosion cracking*, Journal of the Mechanics and Physics of Solids, **146**, 104203, 2021, https://doi.org/10.1016/j.jmps.2020.104203.

17. Z.G. Chen, F. Bobaru, *Peridynamic modeling of pitting corrosion damage*, Journal of the Mechanics and Physics of Solids, **78**, 352–381, 2015, https://doi.org/10.1016/j.jmps.2015.02.015.

18. J.M. Zhao, S. Jafarzadeh, M. Rahmani, Z.G. Chen, Y.R. Kim, F. Bobaru, *A peridynamic model for galvanic corrosion and fracture*, Electrochimica Acta, **391**, 138968, 2021, https://doi.org/10.1016/j.electacta.2021.138968.

19. S.Q. Fan, C.W. Tian, Y.P. Liu, Z.G. Chen, *Surface stability in stress-assisted corrosion: a peridynamic investigation*, Electrochimica Acta, **423**, 140570, 2022, https://doi.org/10.1016/j.electacta.2022.140570.

20. C.W. Tian, J. Du, S.Q. Fan, Z.G. Chen, *A general electrochemical peridynamic model for corrosion and electrodeposition*, Journal of Electroanalytical Chemistry, **968**, 118512, 2024, https://doi.org/10.1016/j.jelechem.2024.118512.

21. H. Wang, H. Dong, Z.W. Cat, Y.Z. Liu, W.Z. Wang, *Fatigue behaviors of a nickel-based superalloy after hot-corrosion: Experiments and peridynamic simulations*, International Journal of Fatigue, **180**, 108070, 2024, https://doi.org/10.1016/j.ijfatigue.2023.108070.

22. D.J. Bang, A. Ince, E. Oterkus, S. Oterkus, *Crack growth modeling and simulation of a peridynamic fatigue model based on numerical and analytical solution approaches*, Theoretical and Applied Fracture Mechanics, **114**, 103026, 2021, https://doi.org/10.1016/j.tafmec.2021.103026.

23. O. Karpenko, S. Oterkus, E. Oterkus, *Titanium alloy corrosion fatigue crack growth rates prediction: Peridynamics based numerical approach*, International Journal of Fatigue, **162**, 107023, 2022, https://doi.org/10.1016/j.ijfatigue.2022.107023.

24. H. Wang, H. Dong, Z.W. Cat, Y.Z. Liu, W.Z. Wang, *Corrosion fatigue crack growth in stainless steels: A peridynamic study*, International Journal of Mechanical Sciences, **254**, 108445, 2023, https://doi.org/10.1016/j.ijmecsci.2023.108445.

25. Z.X. Huang, *Revisiting the peridynamic motion equation due to characterization of boundary conditions*, Acta Mechanica Sinica, **35**, 972–980, 2019, https://doi.org/10.1007/s10409-019-00860-3.

26. E. Emmrich, O. Weckner, *On the well-posedness of the linear peridynamic model and its convergence towards the Navier equation of linear elasticity*, Communications in Mathematical Sciences, **5**, 851–864, 2007.

27. S.A. Silling, R.B. Lehoucq, *Convergence of peridynamics to classical elasticity theory*, Journal of Elasticity, **93**, 13–37, 2008, https://doi.org/10.1007/s10659-008-9163-3.

28. S.A. Silling, M. Zimmermann, R. Abeyaratne, *Deformation of a peridynamic bar*, Journal of Elasticity, **73**, 173–190, 2003, https://doi.org/10.1023/B:ELAS.0000029931.03844.4f.

29. O. Weckner, G. Brunk, M.A. Epton, S.A. Silling, E. Askari, *Green's functions in non-local three-dimensional linear elasticity*, Proceedings of the Royal Society A: Mathematical, Physical and Engineering Sciences, **465**, 3463–3487, 2009, https://doi.org/10.1098/rspa.2009.0234.

30. Y. Mikata, *Analytical solutions of peristatic and peridynamic problems for a 1D infinite rod*, International Journal of Solids and Structures, **49**, 2887–2897, 2012, https://doi.org/10.1016/j.ijsolstr.2012.02.012.

31. L.J. Wang, J.F. Xu, J.X. Wang, *Static and dynamic Green's functions in peridynamics*, Journal of Elasticity, **126**, 95–125, 2017, https://doi.org/10.1007/s10659-016-9583-4.

32. Z.X. Huang, *The singularity in the state-based peridynamic solution of uniaxial tension*, Theoretical and Applied Mechanics Letters, **8**, 351–354, 2018, https://doi.org/10.1016/j.taml.2018.05.008.

33. J.K. Chen, Y. Tian, X.Z. Cui, *Free and forced vibration analysis of peridynamic finite bar*, International Journal of Applied Mechanics, **10**, 1850003, 2018, https://doi.org/10.1142/S1758825118500035.

34. X.H. Peng, Z.K. Zhou, H.J. Liu, Z.G. Chen, *Evaluating the effects of nonlocality and numerical discretization in peridynamic solutions for quasi-static elasticity and fracture*, Communications in Nonlinear Science and Numerical Simulation, **140**, 108343, 2025, https://doi.org/10.1016/j.cnsns.2024.108343.

35. Z.G. CHEN, X.H. PENG, S. JAFARZADEH, F. BOBARU, *Analytical solutions of peridynamic equations. Part I: transient heat diffusion*, Journal of Peridynamics and Nonlocal Modeling, **4**, 303–335, 2022, https://doi.org/10.1007/s42102-022-00080-7.

36. Y.C. ZHU, *Equations and Analytical Tools in Mathematical Physics*, Springer, 2021.

37. K.M. LIANG, F. LIU, G.Q. MIAO, *Mathematical Methods for Physics*, 4th ed., Higher Education Press, 2010.

Received April 6, 2025; revised version August 1, 2025.
Published online September 12, 2025.